AIAA 80-0119R

Studies of Plane-Front Solidification and Magnetic Properties of Bi/MnBi

R. G. Pirich,* D. J. Larson,* and G. Busch†
Grumman Aerospace Corporation, Bethpage, N. Y.

Eutectic and off-eutectic Bi/MnBi compositions have been directionally solidified parallel, antiparallel, and perpendicular to the gravity vector in a one-*g* environment and in low gravity during the ASTP flight. MnBi rod diameter and interparticle spacing distributions are similar for all gravity vector orientations when grown at high solidification rates in 1 *g*. Previously reported ASTP results are explained by the existence of a metastable magnetic phase and off-eutectic solidification models.

Introduction

THE control of microstructure during crystal growth is strongly dependent on the fundamental processes of heat and mass transfer. Since about 1970 considerable study has focused on the plane-front solidification of eutectic alloys[1] and more recently on thermosolutal convection[2,3] that occurs when the fluid density depends on variables such as temperature and solute concentration. Theoretically, free convection might cause, for example, fluctuations in the rate of solidification[4] which would lead to compositional as well as microstructural variations along the growth direction. In a rodlike eutectic, these variations could lead to changes in volume fraction, rod diameter, interparticle spacing, and electronic properties (e.g., magnetic properties) associated with these microstructural parameters. In addition, for off-eutectic, plane-front directional solidification, the composition is a sensitive function of the magnitude of gravitational force (through the mass transfer film thickness),[5] leading to large compositional changes as a function of fraction solidified.[6] Changes in composition could lead to interface instabilities[7] and non-cooperative growth over a certain fraction of the solidified material.

In order to assess the role of convection and coupled convective diffusive transport on the crystal growth of eutectic alloys, the plane-front solidification of Bi/MnBi during ground-base SPAR experiments and ground-base and flight ASTP experiments has been investigated. The Bi/MnBi eutectic was chosen because its microstructure is characterized by a regular rod eutectic morphology when grown by plane-front solidification with cooperative growth and because one of its components, MnBi, is ferromagnetic. Since the magnetic observables are very sensitive to crystal and morphological structure and can be measured quite precisely, they provide an efficient measurement of the effect of solidification processing.

The intent of the ASTP experiment was to determine if the low-*g* environment would affect solidification processing and resultant magnetic and microstructural properties of eutectic Bi/MnBi. Magnetic analysis of comparably processed flight and ground-base samples indicated that the intrinsic coercivity ${}_mH_c$ and remanent magnetization M_r of the flight samples were on the order of twice as large as similarly processed ground-base samples. This difference has been resolved by subsequent phase diagram and magnetic properties measurements associated with the ground-base SPAR program.

Presented as Paper 80-0119 at the AIAA 18th Aerospace Sciences Meeting, Pasadena, Calif., Jan. 14-16, 1980; submitted Feb. 7, 1980; revision received Dec. 15, 1980.

*Senior Research Scientist.

†Research Scientist, Metals Science Laboratory, Research Department.

Experimental Procedure

Eutectic samples for the SPAR ground-base program were prepared using commercially pure Mn (99.9 wt %) and high purity Bi (99.999 wt %) which were melted together in an evacuated ($\sim 10^{-5}$ Torr) high purity quartz crucible (1.0-cm i.d.) above 446°C, the temperature at which the stoichiometric MnBi compound forms.[8] The melt was electromagnetically stirred for a period of 16 h to insure homogenization. The Bi-Mn equilibrium phase diagram in the region of the eutectic composition was determined,[9] and the eutectic composition found to be 0.72 ± 0.03 wt % Mn (2.69 ± 0.08 atomic % Mn), rather than the previously reported 0.60 wt % Mn (2.24 atomic % Mn). This is an important point because the supposed eutectic ASTP ground base and flight bulk composition was actually Bi-rich off-eutectic.[10]

Portions of these starting boules were then remelted in a specially designed quartz crucible, and directionally solidified at various furnace velocities ($V = 0.5$-30.0 cm/h) and thermal gradients ($G_L = 40$-130°C/cm) using the Bridgman-Stockbarger method in an automatic directional solidification system (ADSS). The ADSS apparatus consists of a furnace assembly that produces a very controlled thermal gradient between the region of the furnace nichrome heating element and a continuously fluid cooled copper quench block that surrounds a stationary cylindrical crucible. The ampoules were instrumented with very fine chromel-alumel thermocouples (0.004-cm bead diameter) sheathed in MgO insulation and 304 stainless steel (0.025-cm maximum diameter). The temperature profile of the melt and solid were monitored during the solidification processing, and the thermal gradient directly measured. The presence of these thermocouple probes does not appear to perturb the solidification processing either through chemical contamination or heat transfer. A representative thermal profile for a eutectic Bi/MnBi sample grown under solidification conditions of $V = 29.8$ cm/h and $G = 130$°C/cm, where the in-situ thermocouple temperature is plotted as a function of elapsed solidification time, is shown in Fig. 1. The solidification temperature was inferred by noting the temperature at which a discontinuous change in slope or thermal gradient occurred. This discontinuity was a result of a discontinuous change in thermal conductivities between liquid and solid Bi/MnBi.

Samples grown in the ASTP program were 0.58 wt % Mn Bi-rich off-eutectic. Starting material was vacuum cast in a resistance furnace and then housed in a fused silica furnace cartridge. The solidification processing was performed in a

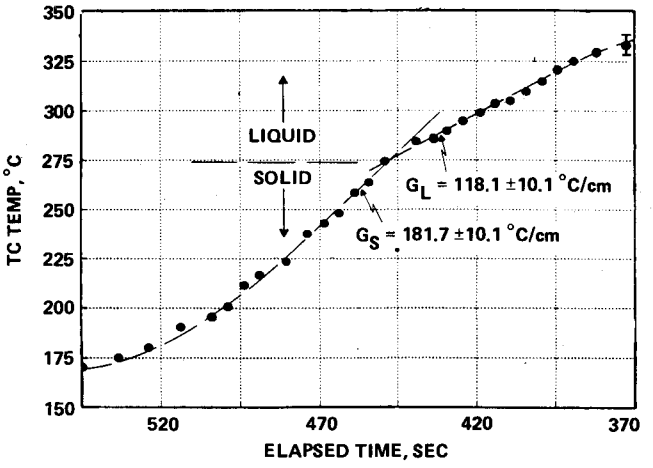

Fig. 1 In-situ thermocouple temperature profile for eutectic Bi/MnBi sample grown at $V = 29.8$ cm/h parallel gravity vector.

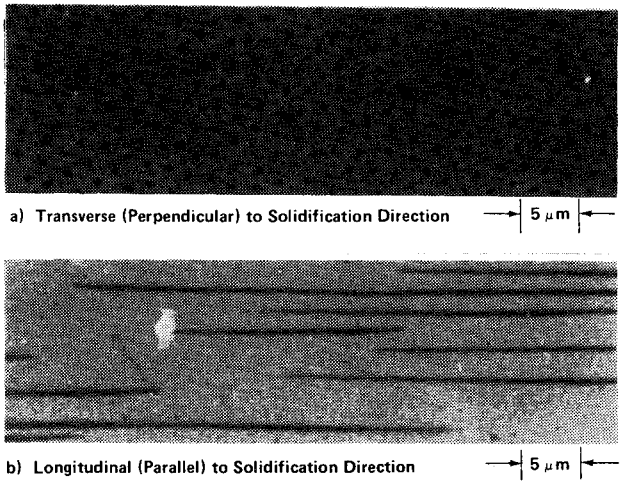

Fig. 2 Optical micrographs showing dispersed MnBi rod morphology transverse and longitudinal to solidification direction.

Westinghouse multipurpose furnace[9] in a 1-g field and aboard the ASTP docking adaptor in a low-g environment. No in-situ thermal measurements were made, and the thermal profiles were deduced from other furnace data.[11] The presumed ASTP solidification processing conditions were $V = 3.0$ cm/h and $G_L = 10.0°$C/cm.[12]

Magnetization of cylindrically shaped samples was measured parallel, perpendicular, and at intermediate angles with respect to the solidification direction as a function of applied field (up to 230 kOe) and temperature (77-533 K) using a vibrating sample magnetometer. These magnetic property measurements were correlated with sample morphology (dispersed MnBi particle size and shape distributions, volume fraction, and rod alignment) as determined from optical micrographs of mechanically polished surfaces analyzed by a computer-aided particle analyzer system.

Results and Discussion

Microstructural Observations

As shown in Fig. 2, plane-front solidification with cooperative growth of eutectic Bi/MnBi results in an aligned ensemble of MnBi rods, with length to diameter ratios ~100, dispersed in a Bi-terminal solid solution ~0.1 wt % Mn. The long axis of the rods is parallel to the solidification direction. The morphology of the rod cross sections is degenerate faceted and chevron shaped at the lowest furnace velocities ($V \leq 3.0$ cm/h), and more circular at higher furnace velocities ($V \geq 20$ cm/h). Mean rod diameters $\langle d \rangle$, as determined by

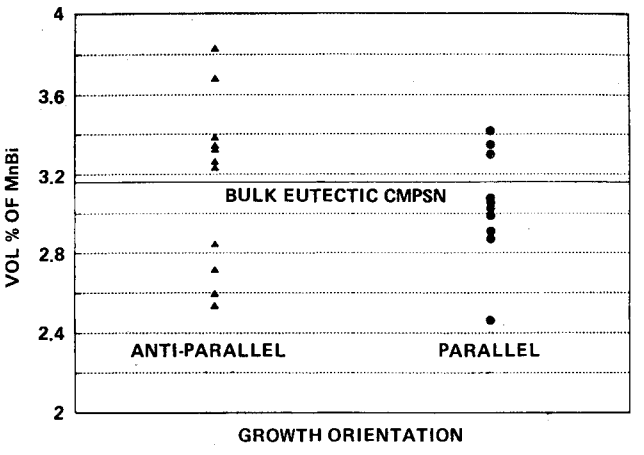

Fig. 3 Measured volume percent distribution of MnBi rods parallel and antiparallel to gravity vector.

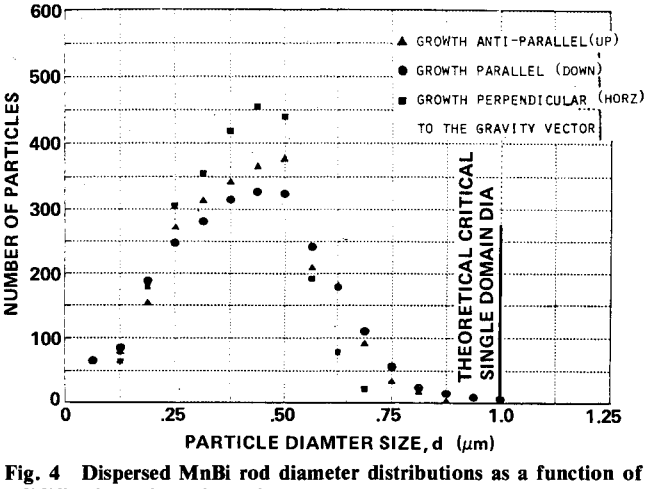

Fig. 4 Dispersed MnBi rod diameter distributions as a function of solidification orientation axis.

fitting the measured rod diameter distributions with a Poisson distribution function and minimizing the χ^2, were found to vary in the expected way with the furnace velocity V, i.e.,

$$\langle d \rangle \sim V^{-1/2} \tag{1}$$

Similar studies by Ravishankar[13] show the same relationship and, in addition, indicate no dependence of the mean rod diameter on thermal gradient.

In the SPAR ground-base studies, samples have been grown parallel, antiparallel, and perpendicular to the gravity field in an effort to change the degree of thermal and solutal convection present. For example, a statistically stable fluid (net fluid density < 0) might be expected for eutectic Bi/MnBi in a growth antiparallel configuration with a sufficiently large temperature gradient since the fluid density of Mn is less than Bi, thereby minimizing convective effects. Similarly, convective flow should be optimum when the growth is perpendicular because both thermal and solutal convection are present. However, as pointed out by Coriell,[3] the interaction of the solute gradient and the temperature gradient on the fluid flow is complex, and a statically unstable density profile without convection as well as a statically stable density profile with convection could occur.

In the high furnace rate regime of $V = 30$ cm/h, there appears to be significant nonhomogeneity in the measured volume fraction of MnBi from area to area, even at the same fraction solidified location. This inhomogeneity is shown in Fig. 3 for samples grown parallel and antiparallel under identical furnace velocity and thermal gradient conditions.

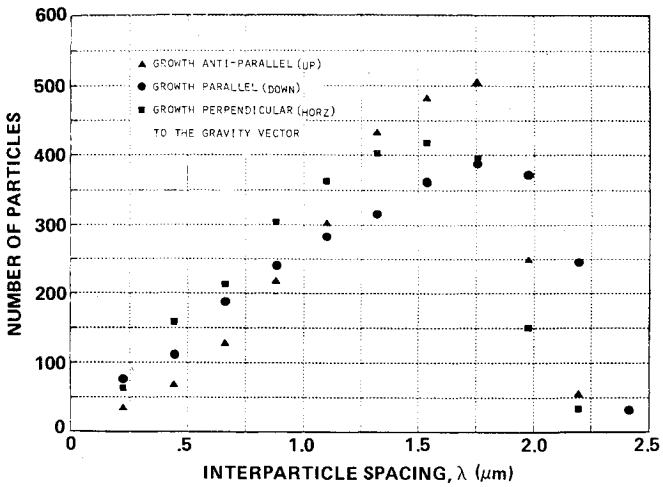

Fig. 5 Interparticle distributions of dispersed MnBi rods measured transverse to solidification direction as a function of growth orientation.

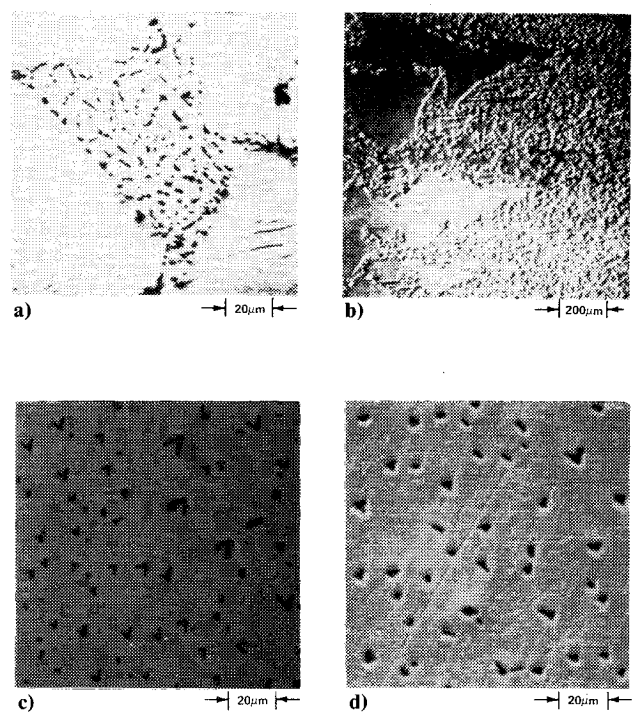

Fig. 6 Observed microstructures of ASTP samples showing macrosegregation in ground base samples (1 *g*); a) primary Bi dendrites and secondary eutectic Bi/MnBi, b) dendritic to aligned transition, c) cooperative plane-front growth, and d) uniform cooperative growth of flight (low-*g*) samples.

Even though the mean volume fraction corresponds to the bulk eutectic composition (~3.18 vol %), the variance in volume fraction is as large as ±25% regardless of growth orientation. Therefore, in comparing rod diameter and interparticle spacing distributions, only a comparison of similar volume fraction areas was made so as not to systematically skew the results. The rod diameter distributions and interparticle spacing distributions for this growth condition are displayed in Figs. 4 and 5, respectively. Each orientation has about the same number of total particles (equivalent volume fractions) and nearly the same mean. However, the skewness of each distribution does change as a function of orientation. For example, both the rod diameter and interparticle spacing distributions indicate that growth parallel has a larger median and asymmetry than growth perpendicular.

In the ASTP program, the observed microstructures for the flight and ground-base samples, as a function of fraction solidified, were strikingly different. For the ground-base samples, the initial fraction solidified region consisted of large primary Bi dendrites with Bi/MnBi eutectic in the interdendrite regions. As shown in Fig. 6a, taken transverse to the solidification direction, the eutectic in this region was not strictly aligned with the solidification direction but was oriented roughly isotropically. As the solidification progressed, the number of primary Bi dendrites decreased and the interdendritic eutectic became better aligned, Fig. 6b, until there was a complete transition from dendritic to aligned cooperative growth as displayed in Fig. 6c. The microstructure of the flight samples, however, showed uniform, cooperative growth from initial to final fraction solidified regions except for very small initial and final transients presumably due to end effects. A representative transverse section at the beginning of solidification is shown in Fig. 6d for a flight sample.

Magnetic Property Observations

It has been shown that plane-front directionally solidified Bi/MnBi with comparable morphologies[14,15] (e.g., mean rod diameter) can differ dramatically in magnetic properties depending on solidification processing conditions and heat treatment after solidification. During the SPAR program, another magnetic phase, other than the expected equilibrium, low temperature (LTP) MnBi phase, which occurs in directionally solidified material, has been identified as the origin of these differences. For samples processed only by directional solidification, the as-grown state, this new magnetic phase, termed the high coercivity or HC phase, is found to coexist with the LTP phase. The HC phase is metastable and transforms to the LTP phase with heat treatment. The amount of transformation depends on the annealing temperature and time. In order to obtain only the LTP MnBi phase, it is necessary to anneal samples of temperatures >200°C for periods up to 24 h. No statistically significant coarsening or change in MnBi rod diameter distribution and bulk rod composition was observed before and after heat treatment as determined from optical microscopy and energy dispersive x-ray analysis. More importantly, the volume percent of HC phase is a sensitive function of solidification processing conditions. For example, by varying the furnace velocity over approximately two orders of magnitude, the amount of HC phase present varies, as shown in Fig. 7, from ~10 to ~100 vol %. In this manner, the magnetic behavior of the HC phase has been isolated.

The HC phase is paramagnetic at room temperature and orders ferrimagnetically between 295 and 77 K with an intrinsic coercivity of ~110 kOe at 77 K, measured parallel to the solidification direction. With the applied magnetic field parallel to the solidification direction, the hysteresis curves corresponding to the LTP and HC phases are distinct and separate (low anisotropy and coercivity for the LTP component, large anisotropy and coercivity for the HC component) with the saturation magnetization of the HC phase (~200 emu/cm^3) lower than that of the LTP phase (~720 emu/cm^3). This behavior is illustrated in Fig. 8 for a SPAR ground-base sample grown antiparallel and containing ~88 vol % HC phase. By assuming that the drop in magnetization $\bar{M}$ near the applied magnetic field $|\bar{H}| = 0$ kOe is attributable to the LTP phase, while the smaller magnetization, larger coercivity loop dropping to zero near $|\bar{H}| = 110$ kOe is the HC phase, we can solve for the resultant magnetization $\bar{M}_i$ at various $\bar{H}_i$ and deconvolute the observed hysteresis curve into two hysteresis curves belonging to the LTP and HC components, respectively. This analysis assumes negligible coupling between the two magnetic phases present, i.e., a magnetically additive composite, and appears to be systematically consistent for all samples studied. Since both phases can be isolated by varying solidification

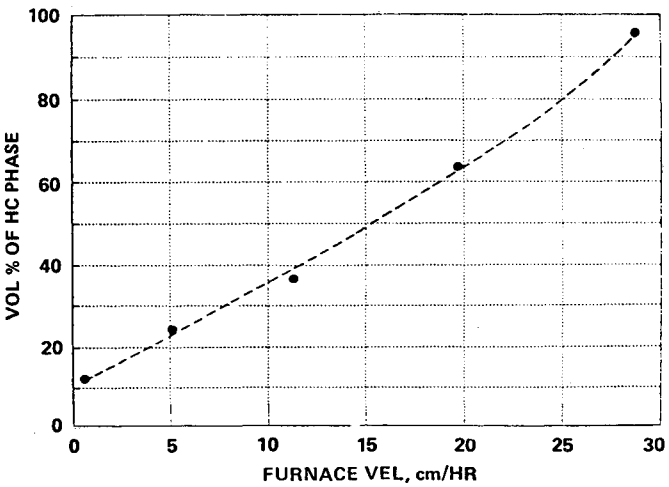

Fig. 7 Volume percent of HC phase as a function of furnace velocity.

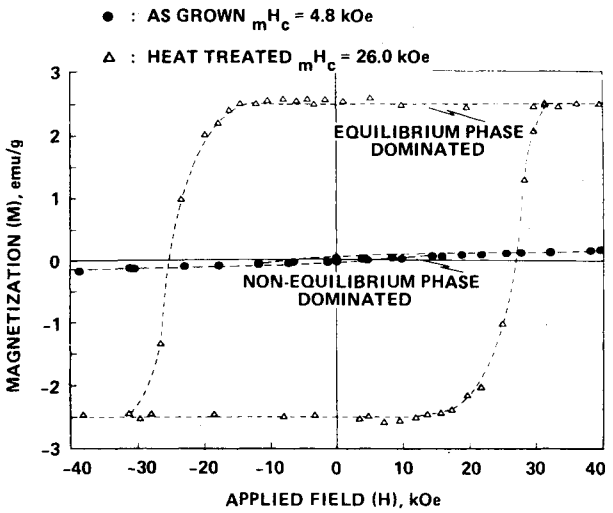

Fig. 9 Hysteresis curve at room temperature.

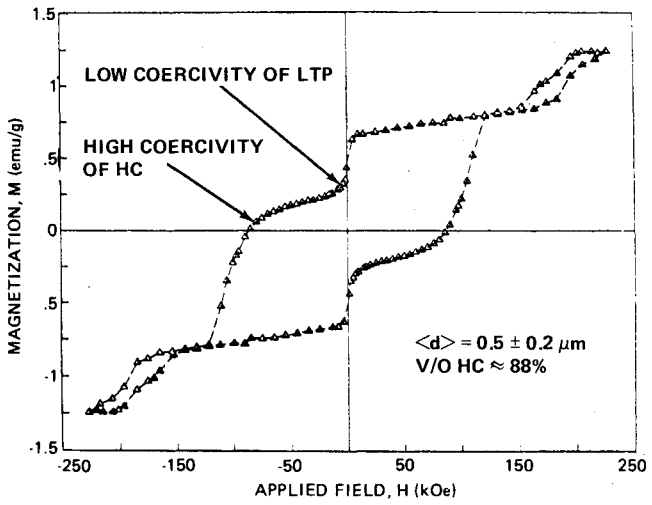

Fig. 8 Hysteresis curve at 77 K for ground base sample.

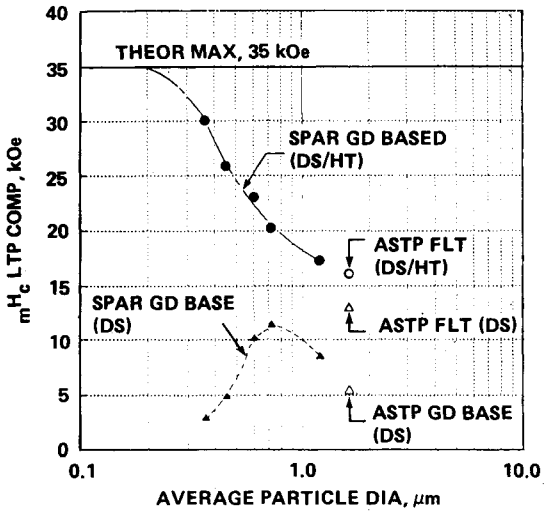

Fig. 10 Dependence of room temperature intrinsic coercivity on mean MnBi rod diameter.

processing parameters and postsolidification heat treatment, the magnetization of each phase normalized to the volume fraction of dispersed MnBi rods was established. Therefore, determining the amount of each magnetic phase present is straightforward. Also seen in Fig. 8 is further magnetic ordering that occurs above 200 kOe. This ordering appears to be incomplete at the highest fields obtained and may be due to the moment reversal of an antiparallel magnetic sublattice in the proposed ferrimagnetic HC structure.[15] Since the HC phase is paramagnetic at room temperature, its influence on the bulk magnetic properties and, specifically, on the LTP component are most dramatically observed at room temperature. As shown in Fig. 9, the coexistence of the HC phase with the LTP phase in the as-grown state reduces the bulk magnetization, but more significantly limits the intrinsic coercivity of the LTP component by introducing regions of lower magneto-crystalline anisotropy where reverse domains can nucleate. As the HC phase transforms to the LTP phase on annealing, the intrinsic coercivity of the LTP component increases as the low anistropy regions decrease until only the equilibrium LTP MnBi phase remains. The effect of rod diameter on the room temperature intrinsic coercivity is shown in Fig. 10. The as-grown samples exhibit a slight increase and then decrease in coercivity as the mean rod diameter decreases. The amount and distribution of HC phase is probably controlling the coercive field for these samples. When the samples have been annealed and contain only the LTP phase, the coercivity increases with decreasing rod diameter over the entire range of particle sizes and approaches the theoretical maximum. The magneto-crystalline anisotropy would appear to be the dominant mechanism.[16] Unfortunately, due to the small MnBi rod cross-sectional area, low volume fraction of dispersed MnBi, and difficulty in chemically separating MnBi rods from the Bi solid solution matrix, no conclusive microstructural and crystallographic evidence has been obtained to date to correlate with observed magnetic properties.

Magnetization as a function of various angles with respect to the solidification direction also was investigated at room temperature. Samples containing combinations of LTP and HC phases, as well as those containing only the LTP phase, were studied as shown in Fig. 11. The expected anisotropy in intrinsic coercivity and remanent magnetization was observed in all samples suggesting that the *c* axis of the hexagonal NiAs structure of LTP MnBi (easy axis of magnetization) lies parallel to the solidification direction regardless of the amount of HC phase present. This was also true for heat-treated samples. It should be noted that the intrinsic coercivity and remanent magnetization are maximum parallel to the long axis of the dispersed MnBi rods and zero perpendicular. Therefore, when the interface stability[7] required for plane-front solidification with cooperative growth is not met, the MnBi rods will no longer be unidirectionally aligned. Such misalignment would result in smaller values for the intrinsic

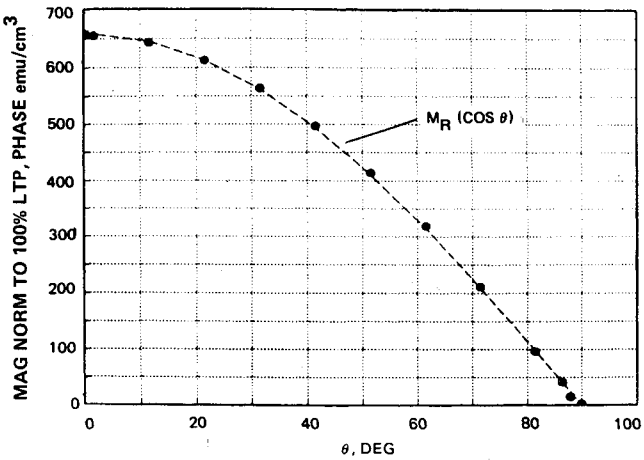

Fig. 11 Remanent magnetization vs solidification direction.

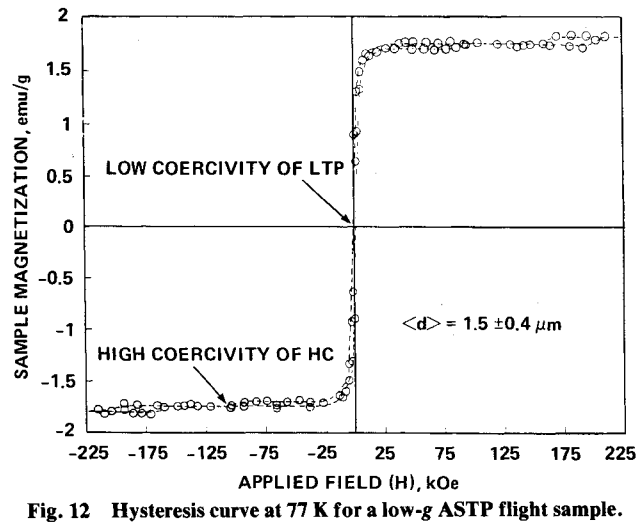

Fig. 12 Hysteresis curve at 77 K for a low-*g* ASTP flight sample.

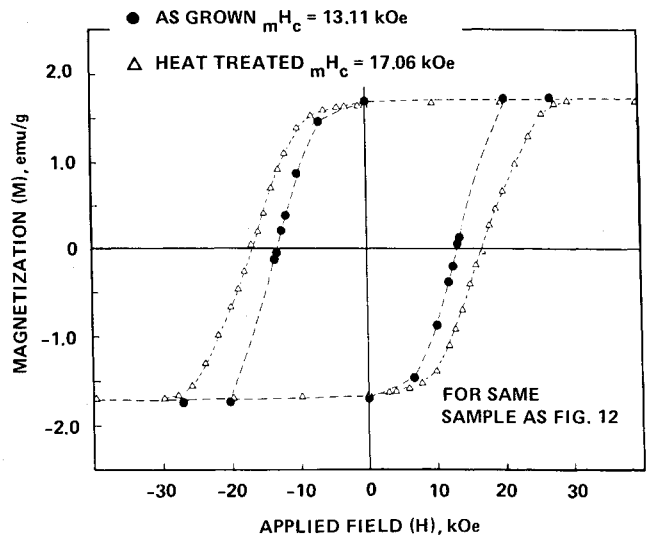

Fig. 13 Hysteresis curve at room temperature.

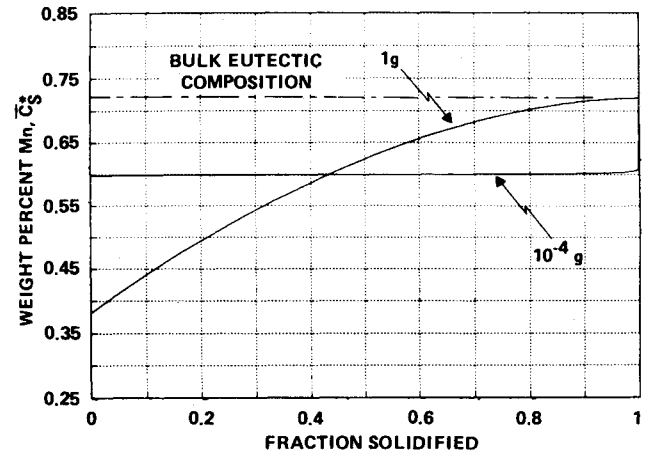

Fig. 14 Final solute distribution for ASTP ground base (1 *g*) and flight (10^{-4} *g*) conditions.

coercivity and remanent magnetization when measured parallel to the solidification direction.

Now turning to the ASTP flight samples. As shown in Fig. 12, the hysteresis curve at 77 K indicates that the flight samples contained <5 vol % of the HC phase. This is supported by measurements at room temperature, displayed in Fig. 13, which show almost no change in bulk magnetization between the as-grown and heat-treated states. The intrinsic coercivity increases slightly after heat treatment in the same manner as the SPAR ground-base samples as shown in Fig. 10. The observed saturation magnetization indicates a composition of 0.58 wt % Mn, and confirms that the ASTP samples were Bi-rich off eutectic. Several pieces, as a function of fraction solidified were also measured and showed the same magnetic properties. This indicates aligned growth over the length of the sample and a uniform composition in agreement with the microstructural observations.

Off-Eutectic Solidification and Interface Stability

According to Mollard and Flemings[7] the condition necessary for plane-front solidification with cooperative growth at off-eutectic compositions is given by

$$G_L/V \geq -m_L[(C_E-\bar{C}_S^*)/D_L] \tag{2}$$

where G_L is the thermal gradient in the liquid at the solidification interface, V the velocity of the solidification interface, m_L the slope of the liquidus at the temperature of solidification, D_L the liquid-diffusion coefficient at the given composition of the melt, C_E the eutectic composition, and C_S the composition of the solid forming. C_S can be related to the bulk composition C_B and convection through the mass transfer film thickness δ_m by

$$(C_B-\bar{C}_S^*)/(C_E-\bar{C}_S^*)=\exp(-V\delta_m/D_L) \tag{3}$$

where,

$$\delta_m=\left(\frac{Pr}{2.41\,Sc}\right)^{1/3}\left\{\left(1+\frac{0.95}{Pr}\right)\Big/ Pr\left[\left(\Delta T\frac{\partial\rho}{\partial T}+\Delta C\frac{\partial\rho}{\partial C}\right)\Big/\rho\nu^2\right]\right\}^{1/4}L^{1/4}ag^{-1/4} \tag{4}$$

and, c is the composition, Δc the composition difference with respect to the eutectic, g the magnitude of the gravitational force, L the characteristic length or diameter of the ampoule, Pr the Prandtl number, Sc the Schmidt number, ΔT the temperature difference in the system, ρ the density, and ν the kinematic viscosity, after Wilcox et al.[5] for solidification perpendicular to the gravity vector assuming a vertical flat plate for simultaneous heat and mass transfer. The only theoretically possible Bridgman-Stockbarger solidification configuration in 1 *g* in which both solutal and thermal convection may be eliminated is a vertical arrangement in which the furnace hot zone is at the top and the solute increases the liquid density for equilibrium partition ratios, $K<1$. For

Bi/MnBi, the Mn solute has a lower fluid density than Bi and thus Bi/MnBi may exhibit solutal instability in a thermally stabilized geometry (growth antiparallel to g with hot zone above cold zone), solutal stability in a thermally destabilized geometry (growth parallel to g with hot zone below cold zone) and both solutal and thermal instability growth perpendicular to g. Preliminary experiments for Bi-rich off-eutectic compositions performed antiparallel, parallel, and perpendicular to g exhibit severe macrosegregation in all cases suggesting that thermal and solutal convection is large enough in Bridgman-Stockbarger growth so that the following equation [Eq. (5)] is applicable.

Using a stagnant film approach, Verhoeven and Homer have described C_S as a function of fraction solidified f for directional solidification in a closed system with forced convection:

$$\bar{C}_S^* = C_E - \frac{(C_E - C_B)}{1 - \exp(-V\delta_m/D_L)} (1-f)^{[+1-\exp(V\delta_m/D_L)]} \quad (5)$$

Using Eqs. (4) and (5), the final solute distribution vs fraction solidified has been calculated for the bulk ASTP composition in the case of $a_g = 980$ cm/s^2 and 980×10^{-4} cm/s^2 and are shown in Fig. 14. The 1-g case demonstrates severe macrosegregation while the composition is uniform for the low-gravity case except for very small initial and final transients. Soret diffusion was ignored because of the growth conditions. A value of D_L of 2×10^{-5} cm^2/s was assumed. It is interesting to note that Eq. (2) is not satisfied under the assumed ASTP flight processing conditions of $G_L = 10°$C/cm and $V = 3.0$ cm/h even though cooperative growth corresponding to the 10^{-4} g case in Fig. 13 was experimentally observed. Either the assumed value for D_L is too small or the assumed ASTP flight processing conditions were somewhat in error resulting in too low a value for G_L/V or both.

During the earlier magnetic properties measurements, the entire lengths of 1-g and low-g samples were compared.[12] Since the 1-g samples contained regions of nonaligned, noncooperative growth, this comparison led to the improvement of the low-g processed samples over those processed in a 1-g environment. Preliminary measurements on selected cooperative growth regions from low-g and 1-g samples show virtually no difference in magnetic properties except for volume fraction differences due to macrosegregation.

Summary

The previously reported[12] magnetic properties improvement between ASTP flight and 1-g samples can be resolved on the basis of convectively driven macrosegregation and the presence of a metastable magnetic phase. As-grown ASTP flight samples were found to have a lower amount of the metastable phase than ground-base samples of comparable morphologies. This difference may be due to the different growth techniques used (Bridgman for ASTP, Bridgman-Stockbarger for SPAR) although the effect of gravity on the formation of this metastable phase is uncertain at this time, and will have to await future SPAR and STS flight experiments.

Acknowledgments

The authors wish to thank P. Adler, J. Papazian, and W. Poit of Grumman; W. Wilcox and P. Ravishankar of Clarkson College; B. Brandt, S. Foner, E. McNiff, and L. Rubin of The Francis Bitter National Magnet Laboratory; and C. Graham of the University of Pennsylvania. This research was partially supported by NASA Contracts NAS8-30577, NAS8-32219, and NAS8-32948.

References

[1] Tiller, W. A., "Liquid Metals and Solidification," American Society for Metals, Cleveland, Ohio, 1958, p. 276.

[2] Turner, J. S., *Buoyancy Effects in Fluids,* Cambridge Press, London, 1973.

[3] Coriell, S. R., Cordes, M. R., Boettinger, W. J., and Sekerka, R. F., unpublished research, June 1979.

[4] Wilcox, W. R., "Effect of Freezing Rate Changes on the Mean Composition of Binary Composites," Aerospace Corp., El Segundo, Calif., Rept. TR-1001 (2250-10)-11, 1967.

[5] Wilcox, W. R., "Simultaneous Heat and Mass Transfer in Free Convection," *Chemical Engineering Science,* Vol. 13, Feb. 1961, pp. 113-119.

[6] Verhoeven, J. D. and Homer, R. H., "The Growth of Off-Eutectic Composites from Stirred Melts," *Metallurgical Transactions,* Vol. 1, Dec. 1970, pp. 3437-3441.

[7] Mollard, F. R. and Flemings, M. C., "Growth of Composites from the Melt-Part I," *Transactions of AIME,* Vol. 239, Oct. 1967, pp. 1526-1533.

[8] Chen, T., "Contribution of the Equilibrium Phase Diagram of the Mn-Bi System Near MnBi," *Journal of Applied Physics,* Vol. 45, May 1974, pp.2358-2360.

[9] Pirich, R. G., Busch, G., Poit, W., and Larson, D. J., "The Bi-NmBi Eutectic Region of the Bi-Mn Phase Diagram," *Metallurgical Transactions A,* Vol. 11A, Jan. 1980, pp. 193-194.

[10] Larson, D. J., "Zero-G Processing of Magnets, ASTP Experiment MA-070 Preliminary Science Report," NASA TXM-58173, Feb. 1976.

[11] "Thermal Analysis of the Apollo Soyuz Test Project MA-070 Experiment in the Flight Environment, Teledyne Brown Engineering," Tech. Letter ASD-EP44-22740 (SO-E0117-PARIII) H72, Jan. 21, 1976.

[12] Larson, D. J., "Zero-G Processing of Magnets, Experiment MA-070," Grumman Research Department, Bethpage, N. Y., Rept. RE-523, Dec. 1976.

[13] Ravishankar, P. S., "Directional Solidification of MnBi-Bi Alloys," Ph.D. dissertation, Clarkson College of Technology, 1979.

[14] Pirich, R. G. and Larson, D. J., "Magnetic and Metallurgical Properties of Directionally Solidified Bi/MnBi Composites: The Effects of Annealing," *Journal of Applied Physics,* Vol. 50, No. 3, March 1979, pp. 2425-2427.

[15] Pirich, R. G., Larson, D. J., and Busch, G., "The Role of Processing Parameters on the Magnetic Properties of Directionally Solidified Bi/MnBi Composites," *IEEE Transactions on Magnetics,* Vol. MAG-15, No. 6, Nov. 1979, pp. 1754-1756.

[16] Brown, W. F., *Micromagnetics,* Interscience, New York, 1963.